water

MDPI

Article

The Morphological Evolution of a Step–Pool Stream after an Exceptional Flood and Subsequent Ordinary Flow Conditions

Giacomo Pellegrini [1], Riccardo Rainato [1,*], Lorenzo Martini [1] and Lorenzo Picco [1,2,3]

[1] Department of Land, Environment, Agriculture and Forestry, University of Padova, 35020 Padova, Italy; giacomo.pellegrini@phd.unipd.it (G.P.); lorenzo.martini.2@phd.unipd.it (L.M.); lorenzo.picco@unipd.it (L.P.)
[2] Faculty of Engineering, Universidad Austral de Chile, Valdivia 5090000, Chile
[3] RINA—Natural and Anthropogenic Risks Research Center, Universidad Austral de Chile, Valdivia 5090000, Chile
* Correspondence: riccardo.rainato@unipd.it; Tel.: +39-0498272695

Abstract: Mountain streams are frequently characterized by step–pool morphology that provides stability and energy dissipation to the channel network. Large flooding events can overturn the equilibrium of the step–pool condition by altering the entire configuration. This work focuses on the impact of the "Vaia" storm (27–30 October 2018) on a step–pool mountain stream (Rio Cordon, Northeast Italy) and on its evolution after two years of ordinary flow conditions. To achieve the aims, this work uses both remote sensing data (LiDAR and UAV) and direct field measurements (i.e., longitudinal profiles and grain sizes distributions) performed pre-event, post-event, and 2 years later (current conditions). The results show a significant widening (width +81%, area +68%) and the creation of a new avulsion after the storm and a substantial change between the number of units (51 in the pre-event, 22 post-event, and 51 in the current conditions) and characteristics of step–pool sequences between pre- and post-conditions. Furthermore, it proves the ongoing processes of morphological stabilization since the current step–pool sequences parameters are heading back to the pre-event values. Such results suggest clear susceptibility of step–pool to exceptional events and fast recovery of such setting during barely two years of ordinary flow conditions.

Keywords: mountain basin; Vaia storm; exceptional flood event; UAV; LiDAR; step–pool evolution; ordinary flow conditions

Citation: Pellegrini, G.; Rainato, R.; Martini, L.; Picco, L. The Morphological Evolution of a Step–Pool Stream after an Exceptional Flood and Subsequent Ordinary Flow Conditions. *Water* **2021**, *13*, 3630. https://doi.org/10.3390/w13243630

Academic Editors: Chang Huang, Guiping Wu and Frédéric Frappart

Received: 22 October 2021
Accepted: 15 December 2021
Published: 17 December 2021

1. Introduction

The morphological configuration of a fluvial system is the result of a complex interplay between different factors. In mountain environment, the latter are mainly constituted by climatic, geological, hydrological, and sedimentological forcings, to which mountain streams have to adapt. To describe and better understand the mountain stream morphology, different classifications were proposed in the literature. Up to now, the most used and shared is the classification proposed by Montgomery and Buffington [1], which defines the streams according to the channel-reach morphologies. These are classified as follows: colluvial, bedrock, cascade, step–pool, plane bed, pool riffle, and dune ripple. Worth adding is the typology "rapids" that was introduced firstly by Church and Zimmermann [2] and then used by Gomi et al. [3]. In this work, particular attention is paid to the step–pool configuration that is one of the most common morphologies in mountain streams [4]. As the name suggests, the step–pool setting is characterized by the presence of an upstream step and a downstream pool. Higher water level upstream and a lower moving downstream characterize the pools. The steps are commonly composed of large boulders or wood logs that imbricate smaller boulders, cobbles or gravels, entailing stability and a heterogeneity in the streambed material. Additionally to the steep slope (>5%), the step–pool setting develops mainly under the conditions of highly heterogeneous grain size, i.e., spanning from fine granules to large boulders [4,5]; near critical to supercritical flows [6]; persisting

limited sediment supply conditions and limited transport rate [5]. This morphology is also known to be a configuration that effectively dissipates energy [7]. Dissipation that is favored by both the grain and form roughness. The former is verified since the large elements provide resistance to the water flow, the latter, instead, occurs due to the presence of the vertical drop of the step that reduces the potential energy, which otherwise would be converted into a longitudinal component of the kinetic energy [8], influencing erosional and sediment transport processes [9]. The mean flow velocity for a step–pool stream, in fact, is the minimum attainable for assigned values of slope, grain size distribution and roughness [4]. The step–pool configuration can be described by a series of descriptive parameters, proposed by Whittaker and Jaeggi [10] and Abrahams and Atkinson [11], i.e., step width (W), step–step drop (Z), step–pool height (H), pool–pool spacing (Lp), step–step spacing (Ls), and mean slope (S). The mean H and mean Ls of a step–pool unit can be used to define the steepness factor [10–12]. Based on field and flume experiments, Abrahams and Atkinson [11] suggested that the maximum resistance to the flow of a step–pool setting is satisfied when the steepness factor is equal to 1.5 S. Furthermore, field experiments by Lenzi [4] demonstrated that such parameter equals 0.79 S when the step–pool configuration faces unstable conditions. The addition of the S parameter to the steepness permits to compute the non-dimensional steepness (c) which gives further information on the slope of the pool bottom profile [4]. Step–pool configuration plays an important role in controlling sediment transport processes and, in the mountain streams' sediment yield. This capacity to influence the sediment transport processes is also used for ecological and management issues. At present, in fact, step–pool settings are used to provide both watershed protection and restoration of mountain fluvial systems. The capacity of step–pool configuration to modulate the sediment fluxes was also proven by study cases that documented its removal. In fact, the suppression of step–pools led to an increase in sediment yields due to the reduction in grains interlocking, and bedform roughness [4,5]. In addition, in highly confined valleys the step–pool configuration can act as a reinforcement of the banks; therefore, its removal may promote hillslope instabilities and the increase in sediment supply [5,13]. As far as the alteration of step–pool is concerned, Crowe [14], through flume experiments, identified several processes such as: burial by sediments, collapse of key elements due to erosion of supporting fine particles, failure due to downstream plunge pool erosion, and collapse due to collision by large particle as processes for which a step can be removed. Nevertheless, the field analysis carried out in the Erlenbach by [5] identified an additional step removal process, consisting in the direct entrainment of key elements due to outstanding hydraulic forcing conditions. Large and infrequent floods are commonly the main causes of mountain streams' morphological alteration expressed as new avulsions [15], channel widening [16], and changes in the streambed configuration [17]. Such morphological changes can be investigated by means of remote sensing approaches relying on LiDAR, UAV, and aerial photos [18–20], which can be integrated by accurate field surveys in order to limit their uncertainty [21,22].

Therefore, in light of the susceptibility of the mountain step–pool streams to a wide range of natural disturbances [23] and given the increase in intensity and frequency of such events, it is of crucial importance understanding their responses and evolutions after flood events of different magnitude. In this sense, the Northeast of Italy was recently affected by the "Vaia storm" (27–30 October 2018), a low-pressure system causing high Scirocco wind gusts (>200 km/h) and cumulative precipitation up to 715 mm [16,24].

This work provides an accurate study about the morphological response of an alpine step–pool stream to a large and infrequent flood, and subsequent ordinary flow conditions. The unique opportunity of analyzing the Vaia storm provides new information concerning the step–pool morphological changes and new tips for future management guidelines in order to predict mountain streams evolution in a future scenario featuring climate change. Therefore, to analyze the event precisely, particular attention is given to: (i) the planimetric evolution, (ii) the alteration of step–pool configuration, and (iii) the grain size variations.

2. Materials and Methods

2.1. Study Area

The Rio Cordon catchment is located in the eastern Alps of Italy, precisely in the Agordino valley (Belluno, Veneto Region) (Figure 1). It has an extension of 5 km^2 and a typical alpine climate. The mean annual precipitation is stable (1986–2018) around 1180 mm [25], whereas the mean annual temperature (T°) has distinctly increased over 1 °C during the last three decades [26]. At present, the mean T° is around 7.5 °C. The nivo-pluvial regime of the basin favors predominant snowfalls in the late fall, during the winter season and in the early spring. In the rest of the year, short and intense rainfalls feature the runoff regime.

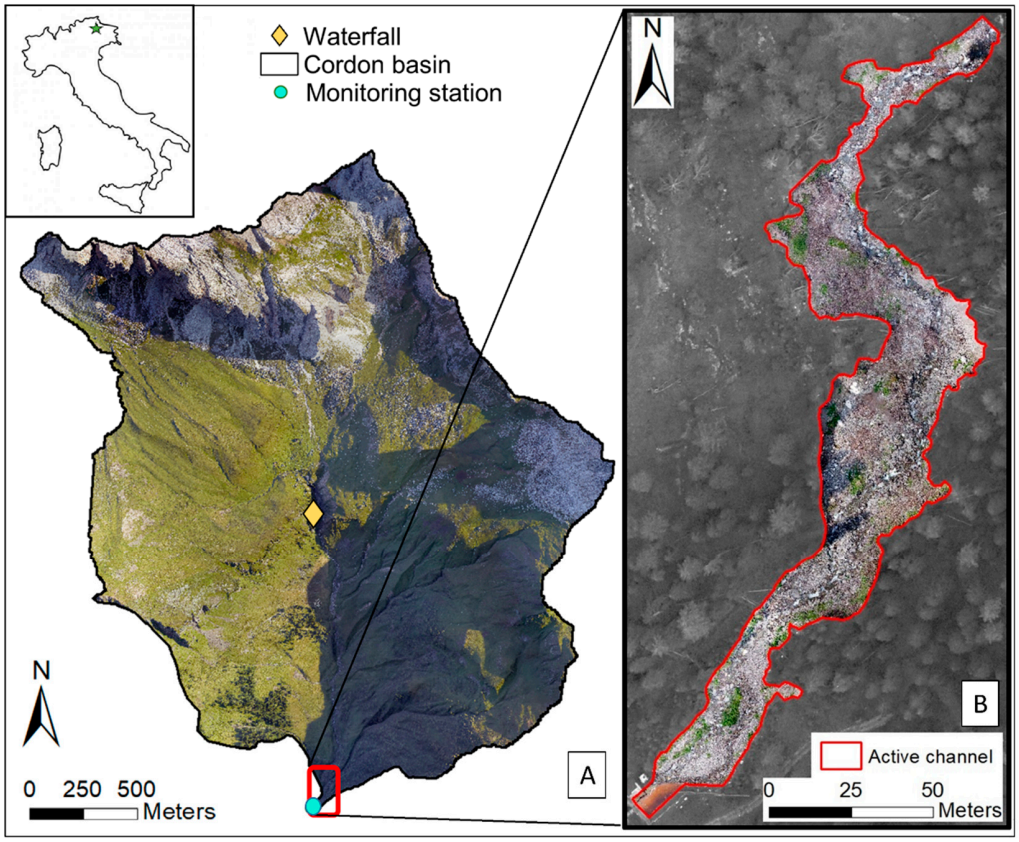

Figure 1. (**A**) Aerial picture of the Rio Cordon basin located in the northeast of Italy (green pentacle), the red square at the outlet of the basin represents the area where the UAV survey was made along the (**B**) study reach. In this part, the planimetric and step–pool analyses were made.

Being part of the Southern Limestone Alps, the substrate of the Rio cordon is characterized by dolomites, limestones, volcanic conglomerates, and calcareous-marly rocks [25]. As the range of elevation goes from 1763 to 2763 m a.s.l., the vegetation cover is limited to 7% of the basin area. The vegetation is composed of spruce (*Picea abies*) and larch (*Larix decidua*). Bare rocks (14%), shrubs (18%), and grasslands (61%), instead, cover the rest of the area. The Rio Cordon main channel (hereinafter Rio Cordon) is characterized by cascade, step–pool, and riffle–pool morphologies [1]. Worth mentioning is the presence of a waterfall just upstream of the middle part of the channel. As it is known [26], such a unit represents a knickpoint and a natural area of disconnection between the upstream and downstream part of the basin. For the lower Rio Cordon, the mean average slope is around 17%. The bankfull discharge is around 2.3 m^3 s^{-1} (Figure 2), which covers a mean channel width of around 5.3 m [26–28]. Thanks to a monitoring program activated since 1985 and based on a permanent measuring station, the Rio Cordon study site can be defined as a "field laboratory". In fact, it was monitored for more than three decades,

allowing for better understanding as to how climatic, hydrological, morphological, and sedimentological dynamics can act in an alpine basin [29–35].

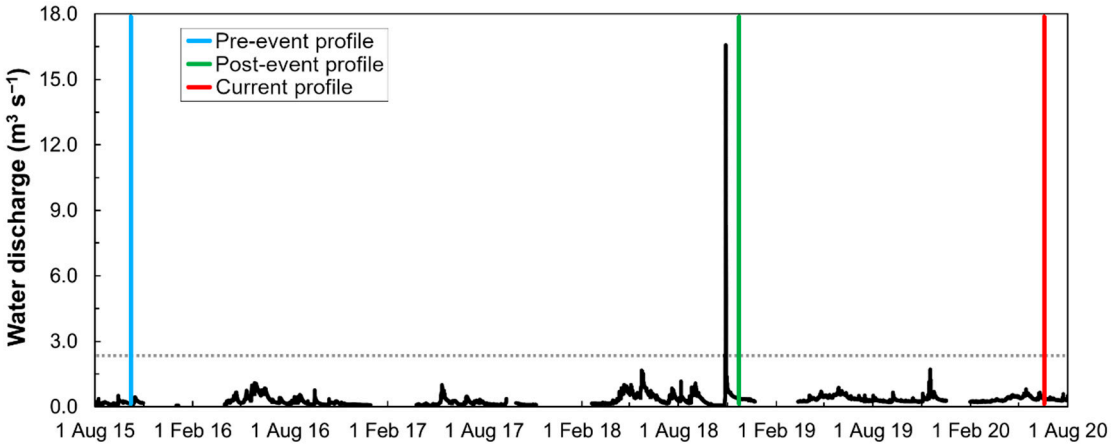

Figure 2. Water discharge experienced by the Rio Cordon during the study period. Until the Vaia storm, the water discharge was measured by the Rio Cordon monitoring station. From Vaia onward, due to the interruption in the monitoring station operations caused by the event, the water discharge acting in the Rio Cordon was determined starting from the Fiorentina Stream discharge and using a specific basin to sub-basin discharge extrapolation. The vertical blue, green and red lines identify the longitudinal profile surveys realized during the pre-event, post-event and the current conditions. The horizontal gray dashed line shows the bankfull discharge (2.30 m^3 s^{-1}).

2.2. Flow Conditions

To analyze the morphological evolution of the study reach channel of the Rio Cordon, three field campaigns were realized in 2015 (pre-event), 2018 (post-event) and 2020 (current conditions), respectively (Figure 2, Table 1). In terms of hydraulic forcing, the period between pre-event and post-event surveys was characterized thanks to the water discharge (Q) recorded by the Rio Cordon monitoring station, which measured Q hourly [32]. In this study period, the Rio Cordon experienced Q mainly under- and near-bankfull flood (Figure 2). However, in October 2018 a severe weather event (hereinafter Vaia storm) affected the study site [36]. Particularly, the heavy rainfall occurred between 27–30 October 2018 (352 mm in ~80 h) triggered a peak of water discharge (Q_P) equal to 16.4 m^3 s^{-1}, i.e., the largest Q_P ever documented in the Rio Cordon [25]. This outstanding hydraulic forcing caused the transport of about 6800 m^3 of bedload to the monitoring station and the consequent interruption of all the operations, included the Q measurements. Therefore, from the Vaia storm, the hydraulic forcing conditions acting in the Rio Cordon had to be derived through indirect methods. To this end, the Q recorded by the nearest gauging station ("Sottorovei" Arpa Veneto station at Fiorentina Stream) was used, through a specific basin to-sub-basin discharge extrapolation [25]. The capacity of the Fiorentina Stream discharge to predict the Rio Cordon discharge was tested and validated by Rainato et al. [25], permitting authors to characterize the Vaia storm flood. In light of this, the relationship between Fiorentina Stream discharge and Rio Cordon discharge was used to describe the hydraulic forcing condition which occurred in the Rio Cordon from October 2018 onward. Figure 2 shows that following the Vaia storm and, in particular, between the post-event field campaign and the survey of current conditions, the Rio Cordon experienced persistent ordinary flows. In this study, we defined as ordinary flow condition the discharge values lower than the bankfull value. Precisely, the peak of water discharge estimated between the pre-event and post-event surveys was equal to 16.4 m^3 s^{-1} (29 October 2018), whereas Q_P = 1.7 m^3 s^{-1} (17 November 2019) was observed between the post-event field campaign and the survey of current conditions.

Table 1. Date and typologies of data used for the analysis.

Data	Pre-Event	Post-Event	Current Conditions
Remote sensing device	LiDAR	LiDAR	UAV
Aerial photos	2015	2019	2020
Digital Elevation Model	2006	2019	2020
Grain Size Distribution	2014	2018	2020
Longitudinal profile	2015	2018	2020

2.3. Planimetric Pattern

The planimetric analysis was carried out taking advantage of three subsequent aerial photos and Digital Elevation Models (hereinafter DEMs) with respect to the pre-event, post-event and current conditions (Table 1). For the first two years (pre-event and post-event) LiDAR surveys were exploited. The ortophotos were characterized by a resolution of 0.20 m with DEMs of 0.50 m. Although the Vaia storm hit the basin in the late 2018, the remote sensing survey was taken the following winter in order to avoid snow covering along the basin area. The remote sensing data of the current conditions, instead, were obtained thanks to Structure from Motion workflow (SfM) [37] using Unmanned Aircraft Vehicles (hereinafter UAVs). Particularly, the drone employed was a quadcopter DJI Phantom 4. The data processing was performed using the Agisoft Photoscan Professional 1.5.5 [38] from which high-resolution aerial photos of 0.02 m and DEM of 0.10 m were produced.

Moving forward, through an aerial photo interpretation technique [26,39], the active channels detected in the pre-event, in the post-event and in the current periods were measured and compared using the Esri ArcMap 10.5 software. Following Lawlor's [40] definition, the active channel considered referred to the geomorphic feature of the torrent which is defined by a break in bank slope and, typically, by the edge of the exposed gravels. The talweg line position was detected via aerial photo interpretation. The combination of the active channel polygon and the talweg position permitted to measure the mean width per each year plotting transversal cross-sections every 20 m.

2.4. Step–Pool Configuration

The analysis of the step–pool configuration was performed surveying the longitudinal profile of the Rio Cordon in the study, which reached 320 m long. This segment partially matches with the 250 m investigated by Lenzi [4], extending for over 70 m upstream. Specifically, the longitudinal profile was surveyed pre-event, post-event and in the current conditions (Figure 2, Table 1). In these surveys, a uniform and consistent approach was used to measure the longitudinal profile. Particularly, a laser rangefinder (horizontal/vertical accuracy = 0.01 m) in conjunction with a target prism was used to measure the relative elevation and distance of each major breaks in the bed topography along the talweg of the Rio Cordon. Using such approach, 335, 149, and 220 points were measured pre-event, post-event, and in the current periods, respectively. Therefore, the mean accuracy achieved was 1.05 points m^{-1} pre-event, 0.47 points m^{-1} post-event, and 0.69 points m^{-1} in the current conditions.

Once obtained the longitudinal profiles, the analysis focused on the identification of step–pool units. A step–pool unit was defined as an accumulation of boulders or large cobbles separating an upstream backwater pool from a downstream plunge pool [2,4,5,41]. According to Lenzi [4], only the step–pools that were part of a sequence of at least three consecutive units were considered. Hence, each step–pool unit was characterized in terms of step–pool height (H), step–step drop (Z), step–step spacing (Ls), pool–pool spacing (Lp), and mean slope (S) (Figure 3). H and Z were measured considering the vertical distance, whereas Ls and Lp were defined measuring the slope distance.

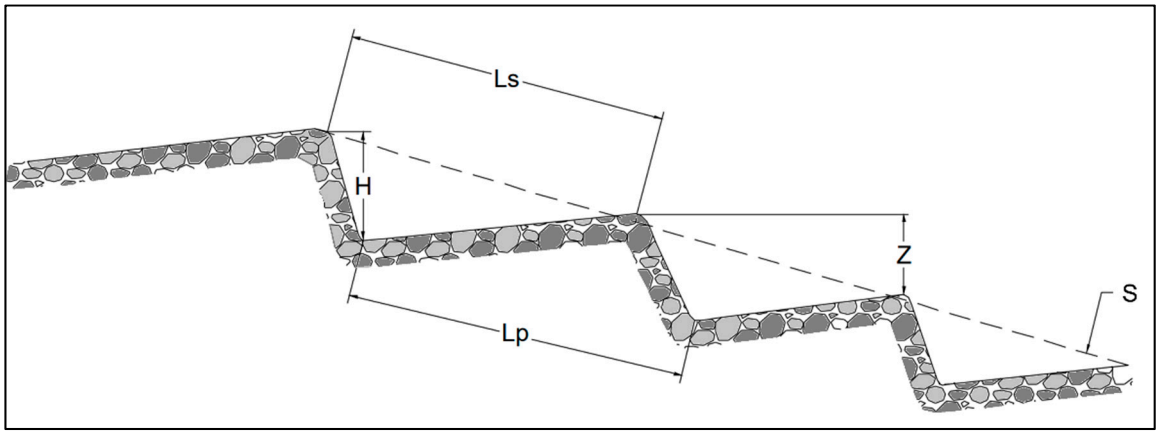

Figure 3. Graphical description of the variables analyzed in the step–pool sequence, i.e., the step–step drop (Z), step–pool height (H), pool–pool spacing (Lp), step–step spacing (Ls), and mean slope (S).

In this sense, only the step–pool units exhibiting H > D_{84} of the pre-event grain size distribution were considered in the analysis (see Section 2.5). The use of D_{84} as minimum threshold is designed to operate an effective identification of the step–pool configuration, relying on sedimentological feature of the study site. The step–pool sequences (SPS) were identified in clusters of three or more consecutive step–pool units, separated upstream and downstream by other channel forms for a distance of at least two times the mean bankfull width (10.6 m). Finally, to compute the steepness and non-dimensional steepness c (see Section 1) the following Equations (1) and (2) were used, according to Lenzi [4] and Abrahams and Atkinson [11]:

$$\text{steepness} = \frac{H}{Ls} \quad (1)$$

$$c = \frac{\frac{H}{Ls}}{S} \quad (2)$$

2.5. Grain Size Distribution Variation

To comprehensively understand the morphological evolution of the Rio Cordon over the study period, the surveys of planimetric variations and step–pool configurations were supported by the definition of the grain size distribution (GSD) of the Rio Cordon surficial material. The GSD analysis were made in the pre-event [42], post-event, and current conditions (Table 1). The three GSD analyses were conducted using the grid by number approach and sampling the surficial in-channel material along the most downstream part of study reach. Specifically, 326, 202, and 229 particles were collected and measured in the pre-event, post-event, and current periods, respectively.

3. Results

3.1. Planimetric Evolution

In the pre-event condition, the Rio Cordon active channel (Figure 4A) covered an area of 3238.5 m^2 and was characterized by a mean channel width of around 10 m (Table 2). The talweg length was 350.8 m.

After the Vaia storm event, the mean channel width and active channel area increased by 81% and 68%, respectively (Figure 4B). Particularly, the former reached a value of 18.6 m whereas the latter registered around 5425.1 m^2. Furthermore, the talweg increased its length to 352.5 m (+0.48%). Compared with the post-event planimetric data, the current conditions exhibited further slight changes (Figure 4C). The channel area increased by 10.5%, covering an active area of 5993.8 m^2. Likewise, the width increased to 20.0 m (+7.5%). On the contrary, the talweg reduced its path by around 1.6%, registering a length equal to 346.8 m.

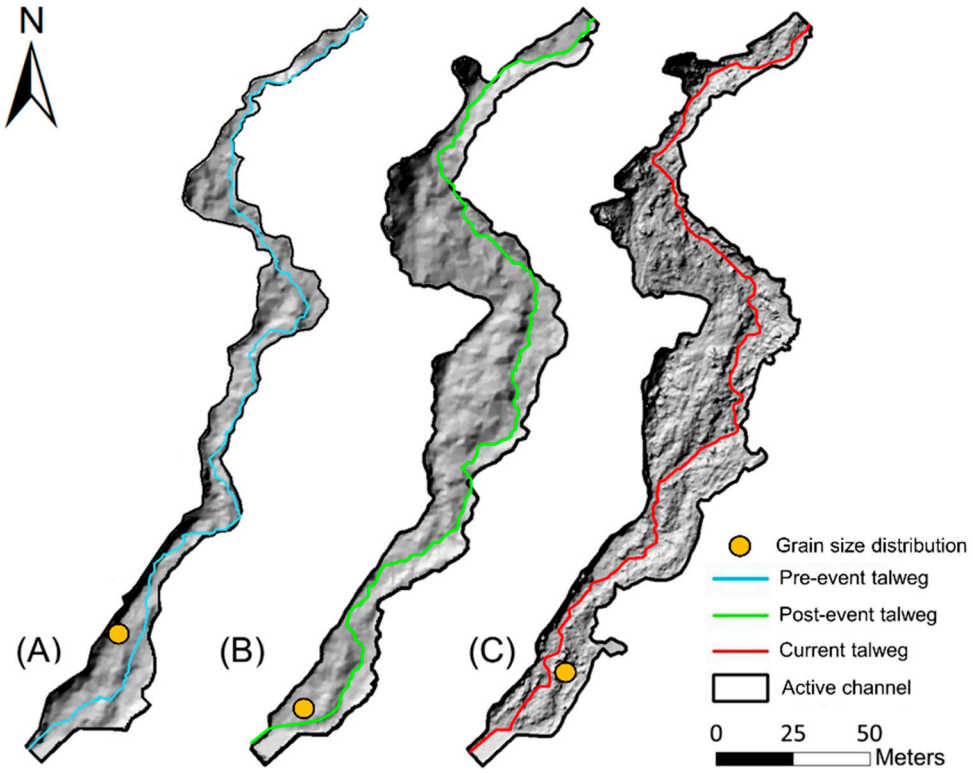

Figure 4. Visual planimetric changes of the active channel and talweg in the (**A**) pre-event, (**B**) post-event and (**C**) current periods. The yellow dot identifies the area where the grain size analysis was realized.

Table 2. Planimetric evolution of the study reach.

	Talweg Lenght	Mean channel Width	Active Channel Area
	(m)	(m)	(m^2)
Pre-event	350.8	10.3	3238.5
Post-event	352.5	18.6	5425.1
Current conditions	346.8	20.0	5993.8

Worth to mention, is the creation of an avulsion around 110 m upstream the outlet of the basin. Such area (Figure 5) affected around 23.3% of the post-event talweg length. Specifically, the avulsion measures 82.3 m and reduced the pre-event talweg length in that area by around 6 m (from 88.5 to 82.3 m).

3.2. Evolution of Step–Pool Configuration

The number of step–pool units identified in the pre-event, post-event, and current conditions was 51, 22, and 51, respectively. All investigated parameters exhibited a similar behavior over the study period, with larger Ls, Lp, H, and Z in the post-event than in the pre-event situation. Hence, in the current conditions, these parameters showed a general decrease, returning to values very close to those observed in the pre-event (Figure 6).

A certain trend is observable also clustering the step–pool units in sequences (SPS, see Section 2.4). In the pre-event, in fact, six step–pool sequences were found, whereas post-event they decreased to 4. In the current conditions, instead, the sequences moved up to 8 (Table 3). Interestingly, the mean Ls, Lp, H and Z observed in the SPS showed, between the pre-event, post-event and the current conditions, a behavior similar to that identified in the units (Figure 6). In fact, the average Ls observed in the step–pool sequences increased from 4.42 m in the pre-event to 6.80 m in the post-event (+53.9%), and then decreased to 4.07 m in the current conditions (−40.2%). The mean Lp increased from 4.36 m to 6.68 m

between the pre-event and post-event period (+53.3%), whereas in the current conditions this was 4.23 m (−36.7%). Similarly, H and Z showed higher mean values in the post-event than in the pre-event, increasing from 0.75 to 0.97 (+30.4%) and from 0.63 to 0.95 (+50.8%), respectively. Therefore, in the current conditions, both H and Z experienced a reduction in mean values, decreasing to 0.75 m (−22.6%) and 0.54 m (−42.8%), respectively (Table 3). Lastly, it is worth noticing that an opposite trend was appreciated in the mean slope of step–pool sequences, which exhibited S equal to 0.14 m m^{-1} in the pre-event period, 0.13 m m^{-1} in the post-event (−5.1%) and 0.15 m m^{-1} in the current conditions (+12.7%).

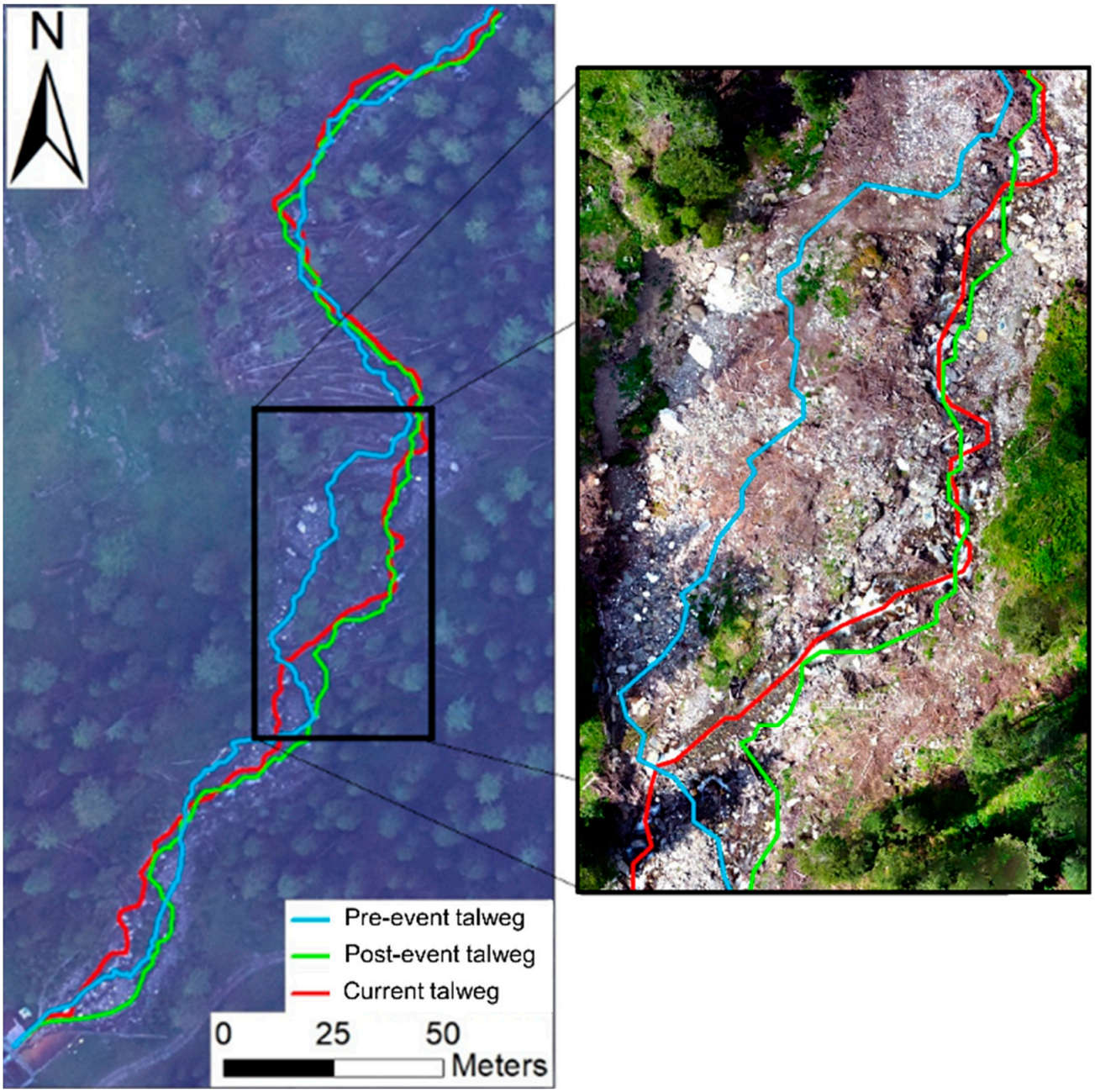

Figure 5. Visual planimetric changes of the talweg for the pre-event, post-event and current conditions. The aerial photo refers to the post-event condition. In the right part, a focus on the new avulsion created during the Vaia storm is shown.

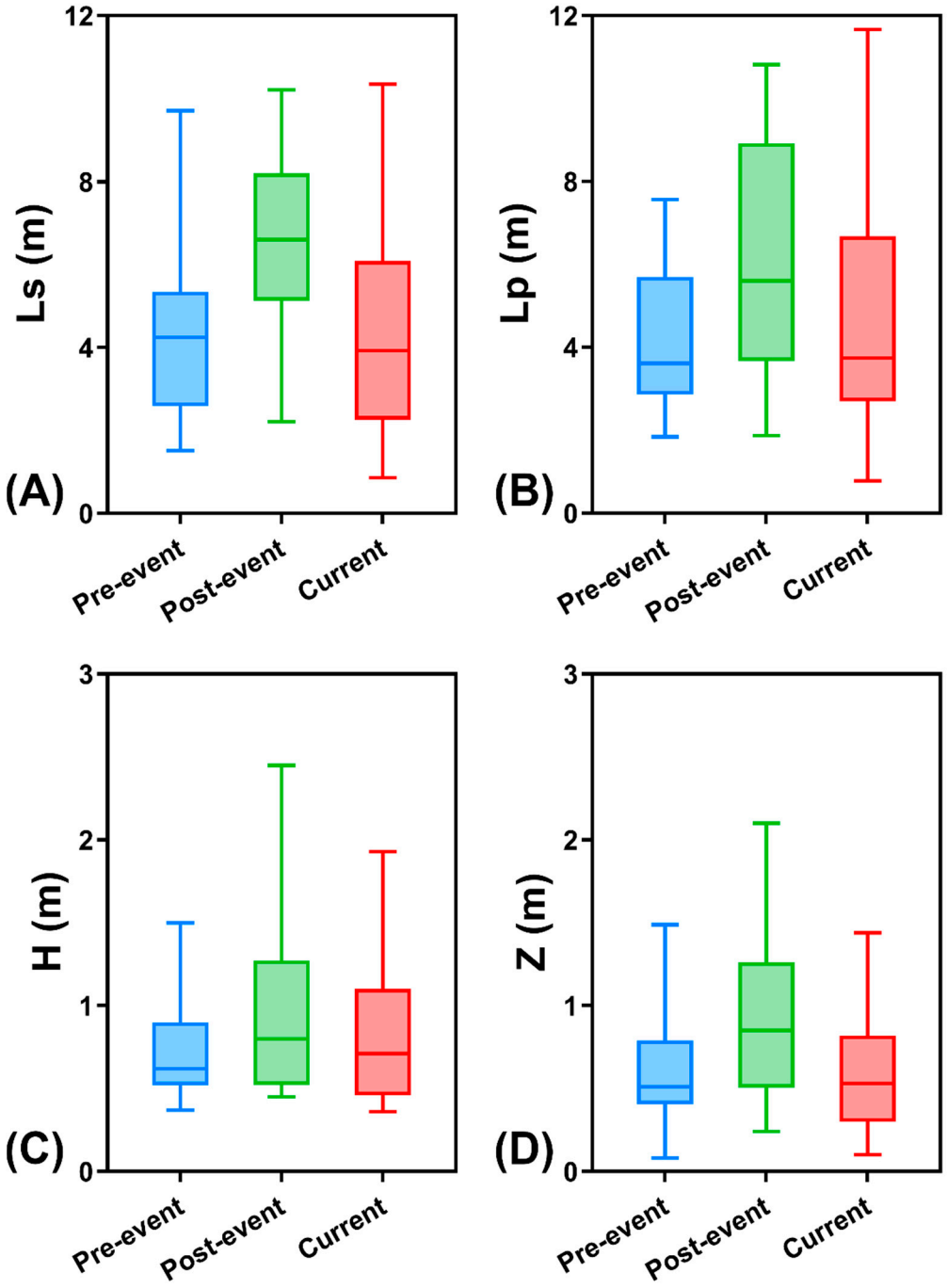

Figure 6. Distribution of (**A**) step–step spacing (Ls), (**B**) pool–pool spacing (Lp), (**C**) step–pool height (H), and (**D**) step–step drop (Z) values in the pre-event, post-event, and current conditions.

The step–pool analysis also permitted to investigate the trend exhibited by the steepness over the study period. Specifically, the relationship between S and mean steepness (H/Ls) for each step–pool sequence was observed pre-event, post-event, and in the current conditions. Figure 7 highlighted that the pre-event and, in particular, the current periods' sequences, fit well the function H/Ls = 1.5 S (maximized flow resistance). Differently, the post-event sequences plot constantly lower. In this sense, the non-dimensional steepness (c) was 1.41 in the pre-event, 1.11 in the post-event, and 1.44 in the current conditions.

Table 3. Mean values of step–step spacing (Ls), pool–pool spacing (Lp), step–pool height (H), step–step drop (Z), and slope of each sequence (SPS) identified pre-event, post-event, and in the current conditions.

		Mean Ls (m)	Mean Lp (m)	Mean H (m)	Mean Z (m)	S (m m^{-1})
Pre-event	SPS1	5.93	5.56	1.03	0.92	0.16
	SPS2	3.04	2.96	0.54	0.39	0.12
	SPS3	4.26	4.36	0.64	0.61	0.14
	SPS4	5.05	4.98	0.70	0.60	0.12
	SPS5	3.98	4.07	0.85	0.71	0.19
	SPS6	4.26	4.24	0.71	0.55	0.12
Post-event	SPS1	7.69	6.61	1.12	1.10	0.14
	SPS2	6.48	7.08	0.86	0.85	0.10
	SPS3	5.98	5.94	0.88	0.84	0.16
	SPS4	7.06	7.10	1.04	1.02	0.14
Current conditions	SPS1	4.06	3.36	0.86	0.64	0.17
	SPS2	5.67	5.63	0.80	0.64	0.12
	SPS3	5.72	6.57	1.04	0.66	0.12
	SPS4	1.52	1.59	0.57	0.37	0.24
	SPS5	2.51	2.23	0.75	0.46	0.19
	SPS6	5.75	6.40	1.12	0.82	0.16
	SPS7	4.04	4.83	0.41	0.29	0.07
	SPS8	3.28	3.23	0.49	0.49	0.14

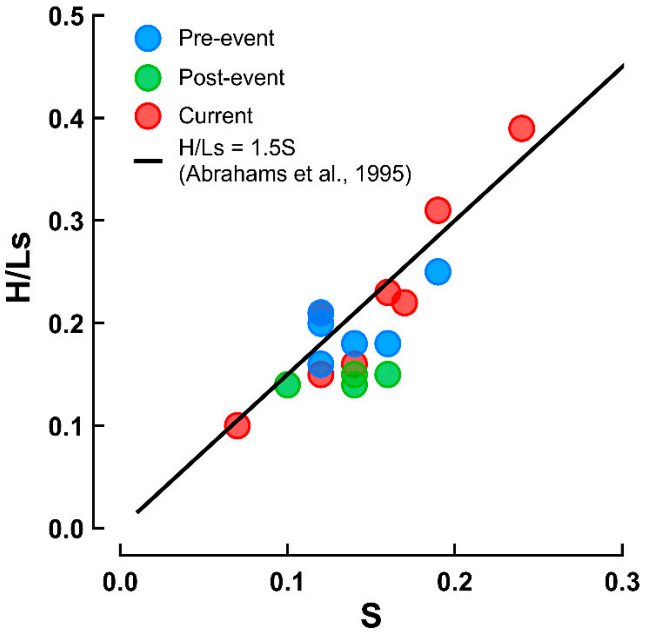

Figure 7. Relationship between S and mean steepness (H/Ls) for each step–pool sequence observed pre-event, post-event, and in the current conditions. Black line is the function H/Ls = 1.5 S, which describes the maximized flow resistance.

3.3. Variation in Grain Size Distributions

Post-event, the grain size distribution of the Rio Cordon surficial material was overall finer than in the pre-event (Figure 8). Particularly, the 16th (D_{16}), 50th (D_{50}), and 84th (D_{84}) percentiles were 29, 114, and 358 mm in the pre-event, decreasing to 26, 78, and 302 mm in the post-event. The GSD measured in the current conditions was comparable to that found post-event (Figure 8). However, D_{16}, D_{50}, and D_{84} equal 24, 76, and 423 mm, suggesting a

certain coarsening of the larger grain size fraction. Such tendency is explicated by the 84th percentile, which increased by 40.1%.

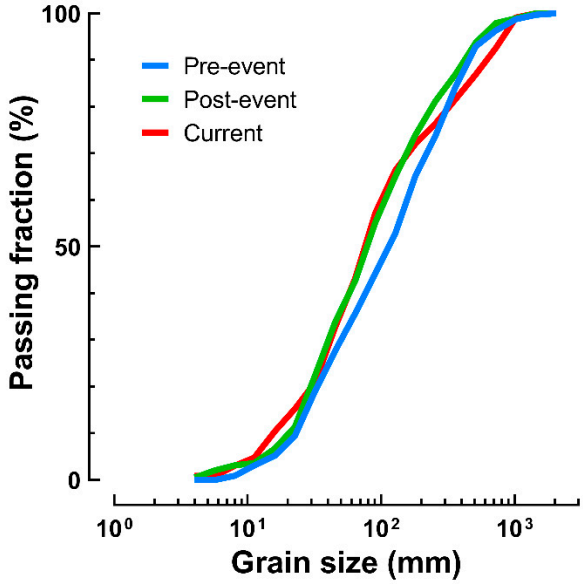

Figure 8. Grain size distributions of Rio Cordon surficial material measured pre-event, post-event, and in the current conditions.

4. Discussion

The pre-Vaia storm conditions, outlined by both the analysis on the pre-event planimetric pattern and GSD are to be considered the results of a long and stable phase of the Rio Cordon distinguished by persistent ordinary hydraulic forcing conditions [43]. In fact, prior to the Vaia storm, the only flood able to significantly modify the Rio Cordon morphology was registered in September 1994. However, this latter event, which registered a Qp = 10.40 m^3 s^{-1}, affected more the hillslope rather than the main channel, creating numerous new sediment source areas [32]. Particularly, since the bedload transport of 1994 flood was around seven times lower than the Vaia flood [25], the stream changed substantially in terms of bedforms configuration but slightly in terms of planimetric pattern. Large planimetric changes, instead, were registered during Vaia, which created an 82.3 m channel avulsion close to the outlet of the basin (Figure 9). In mountain fluvial systems, avulsion channel can be the result of the combination of different factors such as large flooding events and its consequent aggradation effect [44] that triggers the creation of a new and steeper channel [45–47] able to provide new downstream pulses of sediment transport and yield [48]. In the Rio Cordon, such changes go together with the increase in around 80% of the mean channel width and 68% of the channel area. Notwithstanding, the talweg length increased by only 0.48%, featuring a relatively similar planimetric path. The talweg length increase documented in the Rio Cordon was lower than what was experienced by the Erlenbach, consequently to the 50-year flood of June 2007. In fact, such event induced an augment of 3.82% in the Erlenbach talweg length [49]. Interestingly, the increase in mean channel width detected in the Rio Cordon between pre- and post-event was in line with the range +40–105% observed in the mountain Biała River consequently to an 80-year flood [50]. However, it is worth comparing the widening observed in the Rio Cordon with that documented in the Grimmbach and Orlacher Bach after the May 2016 flash flood [20]. In fact, the larger (30 km^2) and flatter (1.5%) Grimmbach mountain basin experienced a mean channel width increase (+590%), clearly higher than the Rio Cordon. Instead, the Orlacher Bach, which features basin area (5 km^2) and stream slope (5.5%) closer to the Rio Cordon, exhibited an increase in mean channel width equal to +210%. In this sense, it is worth noting that the widening in the Rio Cordon was induced by a unit peak discharge equal to 3.3 m^3 s^{-1} km^{-2}, notably lower than the 20.9 m^3 s^{-1} km^{-2} expressed in the

Erlenbach by the June 2007 flood and the 20.0 m^3 s^{-1} km^{-2} experienced by the Orlacher Bach during the May 2016 flash flood, stressing the high geomorphic effectiveness of the Vaia storm in the alteration of main channel. Such hypothesis is supported also by the large variation experienced by the Rio Cordon in terms of active channel area (+68%).

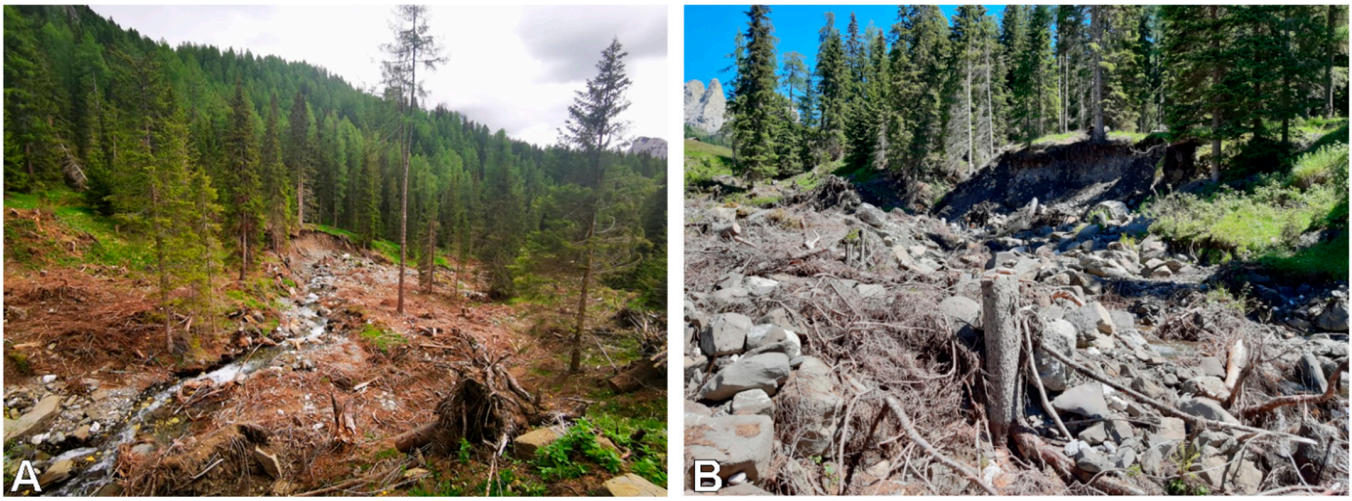

Figure 9. Examples of planimetric changes experienced by the Rio Cordon in the (**A**) middle and (**B**) upstream part of the lower Cordon.

The planimetric changes observed between post-event and current periods resulted one order of magnitude lower than those registered between the pre- and post-event. This result is mainly related to the persistent ordinary flow conditions occurred during the last years (Qp = 1.7 m^3 s^{-1}). However, the capacity of these conditions to further augment the active channel area by 10.5% and the mean channel width by 7.5% seems to suggest that the geomorphic status of the Rio Cordon is still unstable after two years from the Vaia storm. Moreover, the current talweg reduced its length by around 1.6%, implying a certain simplification in the channel path, especially in the downstream part of the study reach (Figure 4C). Interestingly, this result is consistent to what observed in the Erlenbach after 3 years from the large June 2007 flood. During these 3 years (2007–2010), the Erlenbach experienced only ordinary floods, reducing the talweg length by 4.74% and restoring similar values to those of the pre-2007 period [49]. In the Rio Cordon, it is worth mentioning the degree of uncertainty given by the two different techniques of remote sensing data acquisition, precisely between the LiDAR and SfM from UAV technology. Although both provide high-resolution products, SfM DEMs and aerial photos offer lower cell dimension, reducing considerably the possible errors made by the operators in measuring the planimetric features of the channel. On the contrary, LiDAR technology offers more reliability when filtering the water and vegetation cover [51]. In the end, despite the analysis carried out by the same operator, the two different data sources might have affected the results of the present work.

The changes in the planimetric pattern of the Rio Cordon led to the alteration of the step–pool configuration. In this sense, the step–pool investigation realized between the pre-event and the current condition can be compared with the analysis made by Lenzi [4] during the period 1993–1998, offering the rare opportunity to understand how the step–pool configuration can respond to different large floods. Interestingly, the increase observed in Ls (+53.9%), Lp (+53.3%), and H (+30.4%) after the Vaia storm was higher than the +22.7%, +36.7%, and +2.1% documented by Lenzi [4] as a consequence of the September 1994 event. This different response can be ascribed to the different magnitude of the two flood events, in particular in terms of flood duration [25]. However, both cases fall within those exceptional floods that [5] highlighted to be able to generate total step–pool alteration. The same authors, in fact, demonstrated that 40- and 50-year floods in the Erlenbach were capable of disrupting the step–pool morphology, whereas a 27-year event produced only a

partial alteration of this bedform configuration. This also matched with [52], who proved that an extreme rainfall event caused the step–pool system failure in the Latnjavagge basin. Particularly, in the Rio Cordon, the removal of the step–pool units by the Vaia storm seems to be attributable to the outstanding hydraulic forcing conditions that produced also boulder mobility [25]. Such conditions suggest that the direct entrainment of the keystone and the impact of these by large particles could have been the main processes by which the steps were removed. Such a hypothesis would support what was documented in the Erlenbach by Turowski et al. [5], as well as the flume experiments made by [53], in which the motion of keystone accounted for 90% of the total step–pool failure events.

The Ls (−40.2%), Lp (−36.7%), and H (−22.6%) variations detected after 2 years from the Vaia storm (current conditions) were in line with those revealed 4 years since the September 1994 event. In fact, in 1998–1999, Lenzi [4] found −36.4% in Ls, −36.7% in Lp, and −19.1% in H. Therefore, these results seem to suggest that after the October 2018 flood, the Rio Cordon is recovering the step–pool configuration faster than after the September 1994 event, likely due to the post-event hydraulic forcing. In fact, the period between the post-event and the current situation was characterized by persistent under-bankfull flows (Qp = 1.7 m^3 s^{-1}). Differently, the post-large flood period (1994–1999) analyzed by Lenzi [4] featured an over-bankfull flood (Qp = 4.7 m^3 s^{-1}) that can have further disturbed the re-establishment of step–pool configuration. In 2020, the decrease in Ls, Lp, H, and Z may also be caused by the large widening experienced by the Rio Cordon, which, combined with the persistent ordinary flow conditions, can have promoted flow velocity reduction over the step–pool units, and then the prevalence of deposition over erosion [54]. This dynamic may have further supported by the large sediment availability characterizing the post-event period. Interestingly, the step–pool responses observed in the Rio Cordon differed from what document in the Erlenbach after the large June 2007 event [49]. In fact, this latter event has not substantially changed the mean step height and the mean step spacing, but strongly increased their variability. Additionally, in 2010, after 3 years of ordinary flow conditions, the Erlenbach step–pool configuration showed an increase of 4.41% and 8.86% in the mean step height and the mean step spacing, respectively. Therefore, the Erlenbach exhibited a different response in terms of step–pool evolution, in particular, in the variations induced by the ordinary flow conditions. This stresses how the step–pool configurations can respond in a complex way to the different hydraulic forcings, especially, if they were previously altered by large flood events. However, the step–pool recovery currently observed in the Rio Cordon is consistent to what found in the Lainbach by Gintz' et al. [55], who noticed the re-established of this bedform configuration two years after an exceptional flood event. In addition, the trend exhibited by the steepness and by the non-dimensional steepness (c) seems to confirm it. Particularly, the decrease in c from 1.41 (pre-event) to 1.11 (post-event) stressed further how the Vaia flood has destabilized the step–pool morphology, which after that event has shown a more disorganized pattern. However, c equal to 1.44 (current conditions) pointed to a return to a more stable bedform configuration, with a c very close to 1.5, i.e., a condition of maximized flow resistance and well-developed armour layer [4,6]. As for the analysis on the planimetric patterns, the results obtained for the step–pool evolution include some uncertainty related to the methodological technique applied. For instance, the post-event longitudinal profile was built on fewer points per meter because it was surveyed in the weeks immediately after the Vaia flood, i.e., in highly unstable streambed conditions and with the presence of over 130 trees uprooted and laying perpendicularly to the main channel that made field activities particularly difficult and dangerous [36]. However, we assume that the survey was good enough to provide information related to the step–pool configurations.

In light of the results achieved, it is evident how Vaia caused an evident expansion of the active channel (mean channel width and mean active channel area), to which the step–pool configuration responded by increasing its spacing (Ls, Lp) and height differences (H, Z). Moreover, the flood event triggered a general fining of surficial material of Rio Cordon (Figure 8). Differently, the persistent under-bankfull flow conditions occurred

after Vaia flood induced no significant variations in the GSD apart from an increase in the coarse fraction of the distribution (>D_{70}). As above-mentioned, even the planimetric pattern responded modestly to 2 years of ordinary flow conditions, which, instead, induced a significant change in the step–pool units and sequences that returned to a configuration very similar to the pre-event. This result seems to suggest that, in the Rio Cordon, the outstanding hydraulic forcing expressed by Vaia were capable to totally altering the fluvial system, whereas the under-bankfull flow conditions occurred after such event acted on the step–pool configuration but not significantly on the streambed grain size and on the planimetric pattern. Such conclusion is in line with [43], who stressed that even low hydraulic forcing conditions can influence the fluvial system, acting in particular on the setting of streambed material. To conclude, in a future scenario, with more frequent extreme events, understanding the primary response of mountain step–pool streams to diverse flood magnitudes will be a major topic in terms of both management strategies and ecological purposes. In this sense, this work offers the rare chance to investigate the morphological response of a mountain step–pool stream to a large and infrequent flood as well as its evolution two years after that event. Furthermore, thanks to a long-term monitoring programme it was possible to compare the results to a previous exceptional flood in the same catchment.

5. Conclusions

This study presents the response of a step–pool mountain stream to an exceptional flood and its evolution during two years of ordinary flow conditions. The results provide evidence of step–pool destruction and recovery. Specifically, the analysis on the planimetric patterns suggested clear changes in both the width and the talweg path of the Rio Cordon. Such consequence led to an in-channel morphological alteration. In fact, significant changes have emerged between the analysis on the pre-event, post-event, and current step–pool configuration. A distinct increased on the value of the step–pool descriptive parameters, as well as a decrease in the number of sequences immediately after the Vaia storm was highlighted. Furthermore, an ongoing process of morphological stabilization after two years from the large disturbance was identified. The data registered concerning Ls, Lp, Z, and H, in fact, are heading back to the pre-event values. Therefore, our results underline that the step–pool morphology can be destroyed only by large exceptional events and can recover even during a 2 year period of ordinary flow conditions.

However, the comparison of the results with worldwide studies concerning step–pool alteration and recovery from large infrequent disturbances highlighted evidence of complex and non-univocal responses. Therefore, further verification of such dynamics is required. We suggest applying future flume and field experiments to both compare and validate such impacts and the cascading processes occurring in a mountain step–pool stream after an exceptional flood event.

Author Contributions: Conceptualization, G.P., R.R., L.M. and L.P.; methodology, G.P. and R.R.; formal analysis, G.P. and R.R.; investigation, G.P., R.R., L.M. and L.P.; data curation, G.P. and R.R.; writing—original draft preparation, G.P. and R.R.; writing—review and editing, G.P., R.R., L.M. and L.P.; supervision, R.R. and L.P. All authors have read and agreed to the published version of the manuscript.

Funding: This research was funded by the University of Padova Research Project "Sediment dynamics in alpine environment: analysis of sediment mobility, propagation velocity and bedload magnitude in high gradient streams" [BIRD185008]. This research has been also partially funded by the Veneto Region in the frame of the project Vaia-Land (OCDPC 558/2018).

Institutional Review Board Statement: Not applicable.

Informed Consent Statement: Not applicable.

Data Availability Statement: The data presented in this study are available on request from the corresponding author.

Acknowledgments: We thank the ARPA Veneto for providing raw rainfall data and discharge measurements of the Fiorentina Stream. We would like to thank Mario Aristide Lenzi for his valuable suggestions and comments. We also thank the British native speaker, Sally J. Booth, who checked the text of the manuscript.

Conflicts of Interest: The authors declare no conflict of interest.

References

1. Montgomery, D.R.; Buffington, J.M. Channel-Reach Morphology in Mountain Drainage Basins. *GSA Bull.* **1997**, *109*, 596–611. [CrossRef]
2. Church, M.; Zimmermann, A. Form and stability of step-pool channels: Research progress. *Water Resour. Res.* **2007**, *43*, 1–21. [CrossRef]
3. Gomi, T.; Sidle, R.C.; Woodsmith, R.D.; Bryant, M.D. Characteristics of channel steps and reach morphology in headwater streams, southeast Alaska. *Geomorphology* **2003**, *51*, 225–242. [CrossRef]
4. Lenzi, M.A. Step-pool evolution in the Rio Cordon, northeastern Italy. *Earth Surf. Process. Landf.* **2001**, *26*, 991–1008. [CrossRef]
5. Turowski, J.M.; Yager, E.M.; Badoux, A.; Rickenmann, D.; Molnar, P. The impact of exceptional events on erosion, bedload transport and channel stability in a step-pool channel. *Earth Surf. Process. Landf.* **2009**, *34*, 1661–1673. [CrossRef]
6. Comiti, F.; Cadol, D.; Wohl, E. Flow regimes, bed morphology, and flow resistance in self-formed step-pool channels. *Water Resour. Res.* **2009**, *45*, 45. [CrossRef]
7. Chin, A. The geomorphic significance of step–pools in mountain streams. *Geomorphology* **2003**, *55*, 125–137. [CrossRef]
8. Chin, A.; Solverson, A.P.; O'Dowd, A.P.; Florsheim, J.L.; Kinoshita, A.M.; Nourbakhshbeidokhti, S.; Sellers, S.M.; Tyner, L.; Gidley, R. Interacting geomorphic and ecological response of step-pool streams after wildfire. *GSA Bull.* **2019**, *131*, 1480–1500. [CrossRef]
9. Marston, R.A. The Geomorphic Significance of Log Steps in Forest Streams. *Ann. Assoc. Am. Geogr.* **1982**, *72*, 99–108. [CrossRef]
10. Whittaker, J.G.; Jaeggi, M.N.R. Origin of Step-Pool Systems in Mountain Streams. *J. Hydraul. Div.* **1982**, *108*, 758–773. [CrossRef]
11. Abrahams, A.D.; Li, G.; Atkinson, J.F. Step-Pool Streams: Adjustment to Maximum Flow Resistance. *Water Resour. Res.* **1995**, *31*, 2593–2602. [CrossRef]
12. Davies, T.R.; Sutherland, A.J. Resistance to flow past deformable boundaries. *Earth Surf. Process. Landf.* **1980**, *5*, 175–179. [CrossRef]
13. Schuerch, P.; Densmore, A.L.; McArdell, B.W.; Molnar, P. The influence of landsliding on sediment supply and channel change in a steep mountain catchment. *Geomorphology* **2006**, *78*, 222–235. [CrossRef]
14. Crowe, J.C.; Wilcock, P.R. An experimental study of the step-pool bedform. In *Proceedings of the AGU Fall Meeting Abstracts, San Francisco, CA, USA, 6–10 December 2002*; American Geophysical Union: Washington, DC, USA, 2002; Volume 2002, p. H21G-01.
15. Valenza, J.M.; Edmonds, D.A.; Hwang, T.; Roy, S. Downstream changes in river avulsion style are related to channel morphology. *Nat. Commun.* **2020**, *11*, 2116. [CrossRef]
16. Pellegrini, G.; Martini, L.; Cavalli, M.; Rainato, R.; Cazorzi, A.; Picco, L. The morphological response of the Tegnas alpine catchment (Northeast Italy) to a Large Infrequent Disturbance. *Sci. Total. Environ.* **2021**, *770*, 145209. [CrossRef]
17. Wyżga, B.; Liro, M.; Mikuś, P.; Radecki-Pawlik, A.; Jeleński, J.; Zawiejska, J.; Plesiński, K. Changes of fluvial processes caused by the restoration of an incised mountain stream. *Ecol. Eng.* **2021**, *168*, 106286. [CrossRef]
18. Picco, L.; Ravazzolo, D.; Rainato, R.; Lenzi, M.A. Characteristics of fluvial islands along three gravel bed-rivers of North-Eastern Italy. *CIG* **2014**, *40*, 53. [CrossRef]
19. Tonon, A.; Picco, L.; Rainato, R. Test of methodology for developing a large wood budget: A 1-year example from a regulated gravel bed river following ordinary floods. *Catena* **2018**, *165*, 115–124. [CrossRef]
20. Lucía, A.; Schwientek, M.; Eberle, J.; Zarfl, C. Planform changes and large wood dynamics in two torrents during a severe flash flood in Braunsbach, Germany 2016. *Sci. Total. Environ.* **2018**, *640–641*, 315–326. [CrossRef]
21. Messenzehl, K.; Hoffmann, T.; Dikau, R. Sediment connectivity in the high-alpine valley of Val Müschauns, Swiss National Park—Linking geomorphic field mapping with geomorphometric modelling. *Geomorphology* **2014**, *221*, 215–229. [CrossRef]
22. Misset, C.; Recking, A.; Legout, C.; Bakker, M.; Bodereau, N.; Borgniet, L.; Cassel, M.; Geay, T.; Gimbert, F.; Navratil, O.; et al. Combining multi-physical measurements to quantify bedload transport and morphodynamics interactions in an Alpine braiding river reach. *Geomorphology* **2020**, *351*, 106877. [CrossRef]
23. Robson, B.J.; Chester, E.T.; Mitchell, B.D.; Matthews, T.G. Disturbance and the role of refuges in mediterranean climate streams. *Hydrobiologia* **2013**, *719*, 77–91. [CrossRef]
24. Lucianetti, G.; Mastrorillo, L.; Mazza, R.; Partel, P. Groundwater response to precipitation extremes: The case of the "Vaia" storm (Eastern Italian Alps). *Acque Sotter. Ital. J. Groundw.* **2019**, *8*, 39–45. [CrossRef]
25. Rainato, R.; Martini, L.; Pellegrini, G.; Picco, L. Hydrological, geomorphic and sedimentological responses of an alpine basin to a severe weather event (Vaia storm). *Catena* **2021**, *207*, 105600. [CrossRef]
26. Rainato, R.; Picco, L.; Cavalli, M.; Mao, L.; Neverman, A.J.; Tarolli, P. Coupling Climate Conditions, Sediment Sources and Sediment Transport in an Alpine Basin. *Land Degrad. Dev.* **2018**, *29*, 1154–1166. [CrossRef]
27. Lenzi, M.; Mao, L.; Comiti, F. Effective discharge for sediment transport in a mountain river: Computational approaches and geomorphic effectiveness. *J. Hydrol.* **2006**, *326*, 257–276. [CrossRef]

28. Rainato, R.; Mao, L.; Picco, L. Near-bankfull floods in an Alpine stream: Effects on the sediment mobility and bedload magnitude. *Int. J. Sediment Res.* **2018**, *33*, 27–34. [CrossRef]
29. D'Agostino, V.; Lenzi, M.A. Bedload transport in the instrumented catchment of the Rio Cordon: Part II: Analysis of the bedload rate. *Catena* **1999**, *36*, 191–204. [CrossRef]
30. Comiti, F.; Mao, L.; Wilcox, A.C.; Wohl, E.E.; Lenzi, M.A. Field-derived relationships for flow velocity and resistance in high-gradient streams. *J. Hydrol.* **2007**, *340*, 48–62. [CrossRef]
31. Wilcox, A.C.; Wohl, E.E.; Comiti, F.; Mao, L. Hydraulics, morphology, and energy dissipation in an alpine step-pool channel. *Water Resour. Res.* **2011**, *47*. [CrossRef]
32. Pagano, S.G.; Rainato, R.; García-Rama, A.; Gentile, F.; Lenzi, M.A. Analysis of suspended sediment dynamics at event scale: Comparison between a Mediterranean and an Alpine basin. *Hydrol. Sci. J.* **2019**, *64*, 948–961. [CrossRef]
33. Cazzador, D.O.; Rainato, R.; Mao, L.; Martini, L.; Picco, L. Coarse sediment transfer and geomorphic changes in an alpine headwater stream. *Geomorphology* **2021**, *376*, 107569. [CrossRef]
34. Cazzador, D.O.; Rainato, R.; Cavalli, M.; Lenzi, M.; Picco, L. Integrated analysis of sediment source areas in an Alpine basin. *Catena* **2020**, *188*, 104416. [CrossRef]
35. Rickenmann, D.; D'Agostino, V.; Dalla Fontana, G.; Lenzi, M.; Marchi, L. New Results from Sediment Transport Measurements in Two Alpine Torrents. *IAHS-AISH Publ.* **1998**, *248*, 283–289.
36. Picco, L.; Rainato, R.; Pellegrini, G.; Martini, L.; Lenzi, M.A.; Mao, L. An Extraordinary Event Changed the (Morphological) Appearance of a Famous Alpine Stream. In Proceedings of the River Flow 2020—10th Conference on Fluvial Hydraulics, Delft, The Netherlands, 7–10 July 2020; CRC Press: Boca Raton, FL, USA, 2020; pp. 1653–1658.
37. Iheaturu, C.J.; Ayodele, E.G.; Okolie, C.J. An assessment of the accuracy of structure-from-motion (sfm) photogrammetry for 3d terrain mapping. *Geomat. Landmanagement Landsc.* **2020**, *2*, 65–82. [CrossRef]
38. Rusnák, M.; Sládek, J.; Pacina, J.; Kidová, A. Monitoring of avulsion channel evolution and river morphology changes using UAV photogrammetry: Case study of the gravel bed Ondava River in Outer Western Carpathians. *Area* **2019**, *51*, 549–560. [CrossRef]
39. Guzzetti, F.; Ardizzone, F.; Cardinali, M.; Rossi, M.; Valigi, D. Landslide volumes and landslide mobilization rates in Umbria, central Italy. *Earth Planet. Sci. Lett.* **2009**, *279*, 222–229. [CrossRef]
40. Lawlor, S.M. *Determination of Channel-Morphology Characteristics, Bankfull Discharge, and Various Design-Peak Discharges in Western Montana*; US Geological Survey: Reston, VA, USA, 2004.
41. Pampalone, V.; Di Stefano, C.; Nicosia, A.; Palmeri, V.; Ferro, V. Analysis of rill step–pool morphology and its comparison with stream case. *Earth Surf. Process. Landf.* **2020**, *46*, 775–790. [CrossRef]
42. Rainato, R.; Mao, L.; García-Rama, A.; Picco, L.; Cesca, M.; Vianello, A.; Preciso, E.; Scussel, G.; Lenzi, M. Three decades of monitoring in the Rio Cordon instrumented basin: Sediment budget and temporal trend of sediment yield. *Geomorphology* **2017**, *291*, 45–56. [CrossRef]
43. Rainato, R.; Mao, L.; Picco, L. The effects of low-magnitude flow conditions on bedload mobility in a steep mountain stream. *Geomorphology* **2020**, *367*, 107345. [CrossRef]
44. Ashworth, P.J.; Best, J.L.; Jones, M. Relationship between sediment supply and avulsion frequency in braided rivers. *Geology* **2004**, *32*, 21. [CrossRef]
45. Brizga, S.; Finlayson, B. Interactions between upland catchment and lowland rivers: An applied Australian case study. *Geomorphology* **1994**, *9*, 189–201. [CrossRef]
46. Leenman, A.; Eaton, B. Mechanisms for avulsion on alluvial fans: Insights from high-frequency topographic data. *Earth Surf. Process. Landf.* **2021**, *46*, 1111–1127. [CrossRef]
47. Nanson, G.C.; Knighton, A.D. Anabranching Rivers: Their Cause, Character and Classification. *Earth Surf. Process. Landf.* **1996**, *21*, 217–239. [CrossRef]
48. Sims, A.J.; Rutherfurd, I.D. Management responses to pulses of bedload sediment in rivers. *Geomorphology* **2017**, *294*, 70–86. [CrossRef]
49. Molnar, P.; Densmore, A.L.; McArdell, B.W.; Turowski, J.M.; Burlando, P. Analysis of changes in the step-pool morphology and channel profile of a steep mountain stream following a large flood. *Geomorphology* **2010**, *124*, 85–94. [CrossRef]
50. Hajdukiewicz, H.; Wyżga, B.; Mikuś, P.; Zawiejska, J.; Radecki-Pawlik, A. Impact of a large flood on mountain river habitats, channel morphology, and valley infrastructure. *Geomorphology* **2016**, *272*, 55–67. [CrossRef]
51. Smith, M.W.; Carrivick, J.L.; Quincey, D.J. Structure from motion photogrammetry in physical geography. *Prog. Phys. Geogr. Earth Environ.* **2015**, *40*, 247–275. [CrossRef]
52. Beylich, A.A.; Sandberg, O. Geomorphic Effects of the Extreme Rainfall Event of 20-in the Latnjavagge. *Geogr. Ann. Ser. A Phys. Geogr.* **2005**, *87*, 409–419. [CrossRef]
53. Zhang, C.; Xu, M.; Hassan, M.A.; Chartrand, S.M.; Wang, Z. Experimental study on the stability and failure of individual step-pool. *Geomorphology* **2018**, *311*, 51–62. [CrossRef]
54. Liro, M.; Ruiz-Villanueva, V.; Mikuś, P.; Wyżga, B.; Castellet, E.B. Changes in the hydrodynamics of a mountain river induced by dam reservoir backwater. *Sci. Total. Environ.* **2020**, *744*, 140555. [CrossRef] [PubMed]
55. Gintz', D.; Hassan, M.A.; Schmidt', K.-H. Frequency and Magnitude of Bedload in a Mountain River. *Earth Surf. Process. Landf.* **1996**, *21*, 433–445. [CrossRef]